

VITRANSPAD: VIDEO TRANSFORMER USING CONVOLUTION AND SELF-ATTENTION FOR FACE PRESENTATION ATTACK DETECTION

Zuheng Ming¹, Zitong Yu², Musab Al-Ghadi¹,
Muriel Visani^{1,3}, Muhammad MuzzamilLuqman¹, Jean-Christophe Burie¹

¹ L3i, University of La Rochelle, La Rochelle, France ² CMVS, University of Oulu, Finland

³ School of Information & Communication Technology, Hanoi University of Science and Technology, Vietnam

{zuheng.ming,musab.alghadi,muriel.visani, muhammad_muzzamil.luqman, jcburie}@univ-lr.fr zitong.yu@oulu.fi

ABSTRACT

Face Presentation Attack Detection (PAD) is an important measure to prevent spoof attacks for face biometric systems. Many works based on Convolution Neural Networks (CNNs) for face PAD formulate the problem as an image-level binary classification task without considering the context. Alternatively, Vision Transformers (ViT) using self-attention to attend the context of an image become the mainstays in face PAD. Inspired by ViT, we propose a Video-based Transformer for face PAD (ViTransPAD) with short/long-range spatio-temporal attention which can not only focus on local details with short attention within a frame but also capture long-range dependencies over frames. Instead of using coarse image patches with single-scale as in ViT, we propose the Multi-scale Multi-Head Self-Attention (MsMHSA) architecture to accommodate multi-scale patch partitions of Q, K, V feature maps to the heads of transformer in a coarse-to-fine manner, which enables to learn a fine-grained representation to perform pixel-level discrimination for face PAD. Due to lack inductive biases of convolutions in pure transformers, we also introduce convolutions to the proposed ViTransPAD to integrate the desirable properties of CNNs by using convolution patch embedding and convolution projection. The extensive experiments show the effectiveness of our proposed ViTransPAD with a preferable accuracy-computation balance, which can serve as a new backbone for face PAD.

Index Terms— Video-based transformer, multi-scale multi-head self-attention, face presentation attack detection

1. INTRODUCTION

Face Presentation Attack Detection (PAD) [1] is an important measure to prevent spoof attacks for biometric user authentication when using face biometric systems. Many works based on Convolution Neural Networks (CNNs) for face PAD formulate the problem as an image-level binary classification task to distinguish the bona fide from Presentation Attacks (PAs) [2, 3].

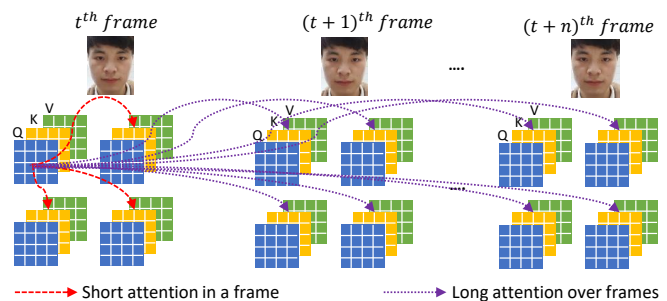


Fig. 1: The short/long-range spatio-temporal attention of the proposed ViTransPAD, which can not only focus on local spatial details with short attention within a frame but also capture long-range temporal dependencies over frames.

The image-based methods are simple and high-efficient. Nevertheless, these methods neglect the context information being useful to improve the generalization performance of face PAD models [4]. Due to the limited receptive field, 3D convolution-based face PAD [5] also suffers from difficulty in learning long-range dependency.

Alternatively, Vision Transformers (ViT) [6] using self-attention to attend the global context of an image is becoming a new mainstream in face PAD [7, 8]. However, ViT is also incapable to model the long-range dependencies over all frames in a video [9].

Inspired by ViT, we propose a Video-based Transformer for face PAD (ViTransPAD) with short/long-range spatio-temporal attention, which can not only focus on local spatial details with short attention within a frame but also model long-range temporal dependencies over frames (see Figure 1). The visualisation of attention maps (in Section 4.5) shows that the proposed ViTransPAD based on short/long-range dependencies can gain a consistent attention being less affected by the noise. Instead of factorizing the spatio-temporal attention [9], we jointly learn spatio-temporal dependencies in our ViTransPAD.

Due to the use of coarse image patches with a single in-

put scale, it is difficult to directly adapt the vanilla ViT to the pixel-level dense prediction tasks such as object detection and segmentation [10] as well as face PAD. To address this problem, we propose the Multi-scale Multi-Head Self-Attention (MsMHSA) architecture to support partitioned multi-scale patches from Q, K, V feature maps to different heads of transformer in a coarse-to-fine manner, which allows to learn a fine-grained representation to perform pixel-level discrimination required by face PAD. Rather than hierarchically stacking multiple transformers as in [10], we simply implement MsMHSA in a single transformer to attain a preferable computation-accuracy balance.

Nevertheless, the pure transformers such as ViT lack some of the inductive biases of convolutions requiring more data to train the models [11] which is not suitable to face PAD training on relative small datasets [12, 13, 14, 15]. To address this problem, we introduce convolutions to our ViTransPAD to tokenize video and employ convolutional projection rather than linear projection to encode Q, K, V feature maps for self-attention. The integrated CNNs force to capture the local spatial structure which allows to drop positional encoding being crucial for pure transformers.

To summarize, the main contributions of this work are: 1) The design of a Video-based Transformer for face PAD (ViTransPAD) with short/long-range spatio-temporal attention. 2) A Multi-scale Multi-Head Self-Attention (MsMHSA) implemented on single transformer allowing to perform pixel-level fine-grained classification with good computation-accuracy balance for face PAD. 3) The introduction of convolutions to proposed ViTransPAD to integrate desirable properties. 4) To the best of our knowledge, this is the first approach using video-based transformer for face PAD. The superior performance demonstrates that the proposed ViTransPAD can serve as an effective new backbone for face PAD.

2. RELATED WORKS

Face presentation attack detection. Traditional face PAD methods usually extract hand-crafted descriptors from the facial images to capture the different clues such as liveness clues (including remote photoplethysmography (rPPG)), texture clues and 3D geometric clues to defend against photo print/video replay/3D masks attacks [16]. Then, deep learning based methods using CNNs learn the representations of different clues from the images to distinguish the bona fide from PAs [3, 17]. Recently, ViT using self-attention is becoming a new mainstream in face PAD [7] due to their strong semantic representation capacities to detect PAs. Some methods based on 3D CNNs [5] or 2D CNNs [4, 18, 19] with auxiliary plugging components try to model long-range dependencies for face PAD. However, the limited receptive field of 3D CNNs hinders its capacity to learn long-range context.

Vision transformers. The first work to introduce Transformer [20] to vision domain is Vision Transformers(ViT) [6].

Thanks to self-attention, ViT and the variants [21, 22] show their superiority in image classification and in downstream tasks [23]. However, these image-based vision transformers only consider the spatial attention in a frame without integrating temporal attention over frames. ViViT [9] model the long-range dependencies over frames with pure transformers. In order to introduce inductive bias of convolutions in pure transformers, [11] propose to use embedded convolution patches. Multi-scale patches are applied in hierarchical stacking transformers [10] to adapt vanilla ViT to pixel-level dense prediction tasks. In this work, we design a simple MsMHSA architecture within a single video-based transformer allowing pixel-level fine-grained discrimination to satisfy the requirement of face PAD.

3. METHODOLOGY

3.1. Overall Architecture

An overview of the proposed ViTransPAD is depicted in Figure 2 (a). Unlike hierarchical stacking transformers using multi-scale patches in [10], we only use a single transformer to apply the multi-scale self-attention with different heads in each layer of transformer.

Convolutional token embedding (CTE). Instead of partitioning each frame into patches and then tokenize patches with linear projection layer, we introduce a convolutional layer to tokenize each frame without partition. Given an input video \mathbf{X}_{in} of size $T \times 3 \times H \times W$, the obtained token map is $\mathbf{X}_m \in \mathbb{R}^{T \times C_m \times H_m \times W_m}$, where T is the number of frames.

Convolutional projection (CP). As well as CTE, we use convolutional projection rather than linear projection to encode $\mathbf{Q}/\mathbf{K}/\mathbf{V} \in \mathbb{R}^{T \times C_A \times H_A \times W_A}$ feature maps.

Then the obtained \mathbf{Q} , \mathbf{K} and \mathbf{V} are fed into the proposed Multi-scale Multi-Heads Self-Attention (MsMHSA) module to learn the short/long-range dependencies over frames in a video. The details are described in Section 3.2. Finally, we add Feed-Forward Network (FFN) with Norm layers at the end of transformer. In this work, linear projection layers in FFN are also replaced by convolution layers. As in ViT, an MLP Head is connected to the transformer to generate the classification embeddings \mathbf{Z} for face PAD. Given an input video \mathbf{X}_{in} , the proposed ViTransPAD can be described as:

$$\mathbf{X}_m = \text{CTE}(\mathbf{X}_{in}) \quad (1)$$

$$\mathbf{Q}, \mathbf{K}, \mathbf{V} = \text{CP}(\mathbf{X}_m) \quad (2)$$

$$\mathbf{H} = \text{MsMHSA}(\mathbf{Q}, \mathbf{K}, \mathbf{V}) \quad (3)$$

$$\mathbf{Y} = \mathbf{H} + \mathbf{X}_m \quad (4)$$

$$\mathbf{Z} = \text{MLP}(\text{FFN}(\text{Norm}(\mathbf{Y})) + \mathbf{Y}) \quad (5)$$

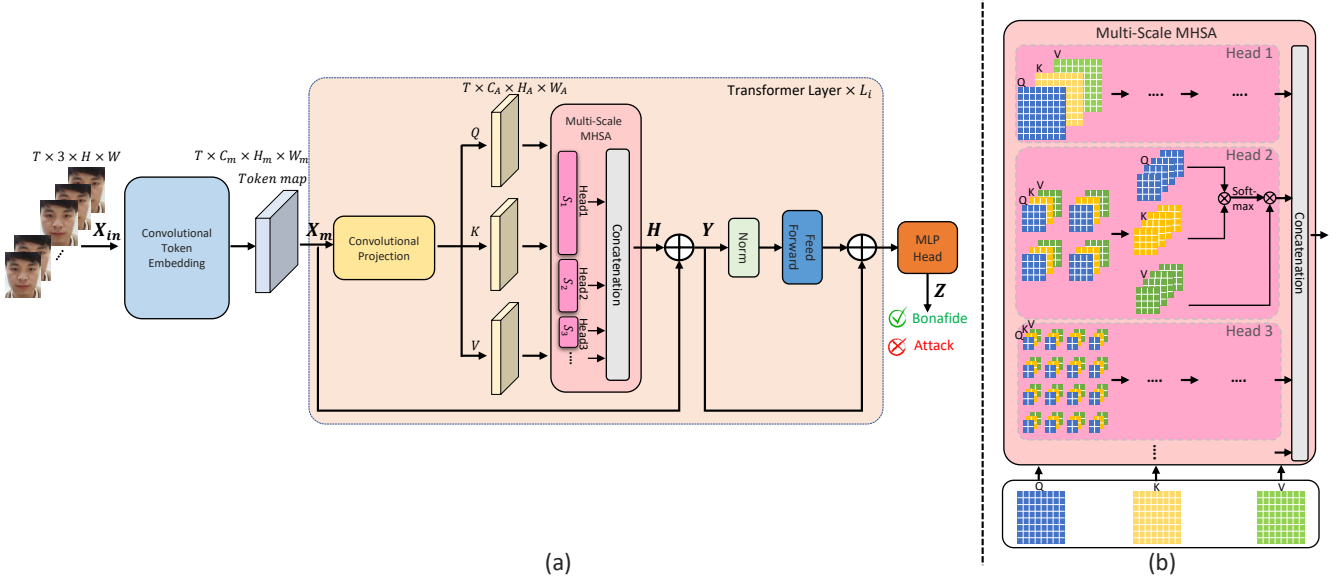


Fig. 2: (a) Overall architecture of the Video-based Transformer for face PAD (ViTransPAD). (b) The proposed Multi-scale Multi-Head Self-Attention (MsMHSA) module in our ViTransPAD.

3.2. Multi-scale Multi-Head Self-Attention (MsMHSA)

The goal of MsMHSA, as shown in Figure 2(b), is to introduce a pyramid structure into the self-attention module to generate multi-scale feature maps which can be used for pixel-level fine-grained image discrimination required by face PAD. The proposed MsMHSA is applied on different heads of each layer of our transformer. All the heads share the similar protocol to calculate the self-attention. In particular, the feature maps $Q/K/V$ are equally divided to each head along the dimension before inputting them to MsMHSA.

Given a transformer with three heads fed by an input feature maps $Q/K/V$ of size $T \times C_A \times H_A \times W_A$, the feature maps for each head are $Q_i/K_i/V_i \in \mathbb{R}^{T \times \frac{C_A}{3} \times H_A \times W_A}$. For the first head $Head_1$, we take a full-size patch $q_1/k_1/v_1 \in \mathbb{R}^{T \times \frac{C_A}{3} \times H_A \times W_A}$ to calculate a global self-attention feature map for the first head $Head_1$. We can obtain the self-attention feature map $h_1 \in \mathbb{R}^{T \times \frac{C_A}{3} \times H_A \times W_A}$ of $Head_1$. Then for $Head_2$, we divide $Q_2/K_2/V_2$ into 2^2 patches, each patch $q_2/k_2/v_2$ of size $T \times \frac{C_A}{3} \times \frac{H_A}{2} \times \frac{W_A}{2}$. We obtain the self-attention feature map $h_2 \in \mathbb{R}^{T \times \frac{C_A}{3} \times \frac{H_A}{2} \times \frac{W_A}{2}}$ of $Head_2$. We continue to divide $Q_3/K_3/V_3$ into 4^2 patches to calculate the self-attention feature map $h_3 \in \mathbb{R}^{T \times \frac{C_A}{3} \times \frac{H_A}{4} \times \frac{W_A}{4}}$ of $Head_3$. Finally, we concatenate the obtained self-attention feature maps $\{h_1, h_2, h_3\}$ to generate the final multi-scale attention feature map $H \in \mathbb{R}^{T \times C_A \times H_A \times W_A}$ in layer L_i (We need to reshape h_2, h_3 to be consistent with h_1):

$$H = \text{Concat}(h_1, \text{Reshape}(h_2), \text{Reshape}(h_3)). \quad (6)$$

The self-attention feature map h_i is given by:

$$h_i = \sum_m^N \sum_n^N \text{Softmax}\left(\frac{q_{i,m} k_{i,n}^T}{\sqrt{d_{head_{i,n}}}}\right) v_{i,n}, \quad (7)$$

where i is corresponding to the i th head $Head_i$, $q_{i,m}$ is the m th patch partitioned from feature map Q_i for the i th head $Head_i$, $k_{i,n}/v_{i,n}$ are the n th patches partitioned from feature maps K_i/V_i for the i th head $Head_i$, then, $q_{i,m}/k_{i,n}/v_{i,n} \in \mathbb{R}^{\frac{C_A}{3} \times \frac{W_A}{l} \times \frac{W_A}{l}}$, $l \in [1, 2, 4]$, and N is the total number of patches of i th head, i.e., $N = T \times l^2$, $l \in [1, 2, 4]$. $d_{head_{i,j}}$ is the dimension of the $q_{i,m}$. For each head $Head_i$, we stack the partitioned patches $q_i/k_i/v_i$ from all frames of a video together to calculate the self-attention feature map of the video (see Figure 2(b)), thus the self-attention of each head $Head_i$ always considers simultaneously the short attention focusing on local spatial information when $q_{i,m}/k_{i,n}$ from the same frame of a video (see the red dotted line in Figure 1 denoting the short attention) and long attention capturing spatio-temporal dependencies over frames when $q_{i,m}/k_{i,n}$ from the different frames (see the violet dotted line Figure 3 denoting the long-range attention). We can also jointly learn the spatio-temporal attention in a unified framework without learning the spatio-temporal attention independently as in [9].

3.3. Loss function for face PAD

Instead of adding a classification token to learn the representation of image as in ViT, we learn the representation of video based on all patch tokens without adding an extra classification token. In practice, the output of MLP Head servers as

the classification embedding \mathbf{Z} in this work (see Figure 2). Then, the learned embedding \mathbf{Z} is input in the cross-entropy loss function to train our model:

$$\mathcal{L}(\mathbf{Z}; \Theta) = \sum_{k=1}^K -y_k \log P(y_k = 1 | \mathbf{Z}, \Theta) \quad (8)$$

where Θ are the parameters of model to be optimized and K is the number of categories, i.e., $K = 2$, which is the classes for face PAD being either bonafide or attack.

4. EXPERIMENTS

4.1. Datasets and setup

Datasets **OULU-NPU (O)** [12], **CASIA-MFSD (C)** [15], **Idiap Replay Attack (I)** [14] and **MSU-MFSD (M)** [13] are used in our experiments. Attack Presentation Classification Error Rate (APCER), Bona Fide Presentation Classification Error Rate (BPCER), Average Classification Error Rate (ACER) [20] and Half Total Error Rate (HTER) [21] are used as evaluation metric in the intra/cross-datasets tests. In intra-dataset test, we follow the evaluation protocols of Oulu-NPU as in [12]. In cross-datasets test, we conduct the evaluation on four datasets **OULU-NPU (O)**, **CASIA-MFSD (C)**, **Idiap Replay Attack (I)** and **MSU-MFSD (M)**. We follow the OCIM protocols proposed in [24] for cross-datasets test in which we randomly choose three of four datasets as source datasets for training the model, and the remaining one is set as the target domain to evaluate the model. So, we have four experimental modes: ‘O&C&I’ to ‘M’, ‘O&M&I’ to ‘C’, ‘O&C&M’ to ‘I’, ‘I&C&M’ to ‘O’.

4.2. Implementation Details

All models are trained on 3 RTX 6000 GPUs with an initial learning rate of $1e-5$ for 200 epochs following the cosine schedule (50 epochs for warmup). Adam optimizer and a mini-batch size of 16 videos (8 frames per video sampled uniformly or with random interval) are applied during training. Data augmentations including horizontal flip and color jitter are used. 224×224 facial images cropped by MTCNN [25] are used for both training and testing models.

4.3. Ablation study

All ablation studies are conducted on the Protocol-2 (different displays and printers between training and testing sets) of OULU-NPU dataset unless otherwise specified.

Effectiveness of convolutions in transformer. demonstrates a good computation-accuracy balance (ACER 1.19% with GFLOPs 7.88) comparing to the pure CNNs or transformer (ViT/ViT(P)), which shows the effectiveness in introducing convolutions into transformers for face PAD. Comparing to convolutional token embedding, ViT is less effective

Table 1: Ablation study on effectiveness of convolutions introduced in transformer (P- Pretrained, T-Transformer).

Model	APCER(%)	BPCER(%)	ACER(%)	#GFLOPs	#Params
CNN	5.43	1.08	3.26	0.63	65M
CNN (P)	2.12	3.30	2.71	0.63	65M
ViT	10.30	4.20	7.25	55.5	86M
ViT (P)	2.38	0.76	1.57	55.5	86M
ViT+T	11.32	6.67	8.99	134.39	87M
ViT (P)+T	5.82	0.94	3.38	134.39	87M
CNN+T	14.60	7.12	10.86	7.88	66M
CNN (P)+T	1.98	0.40	1.19	7.88	66M

Table 2: Ablation study on the proposed Multi-scale MHSA.

28*28	14*14	7*7	ACER(%)
✓			2.81
	✓		2.60
		✓	2.32
✓	✓		1.19
✓		✓	2.06
	✓	✓	2.12
✓	✓	✓	2.30

for tokenizing patches (see ViT+T/ViT(P)+T). The comparison experiments also show that the pretraining (denoted as P) is quite important for face PAD especially for the transformer-based architectures.

Effectiveness of multi-scale MHSA. From Table 2, we can see that all of the results using multi-scale patches are better than the ones using single-scale patch. The best result is achieved when using multi-scale patches of size 28×28 and 14×14 . However, the performance degrades when applying all three patches, which may be due to the overfitting on relative small dataset.

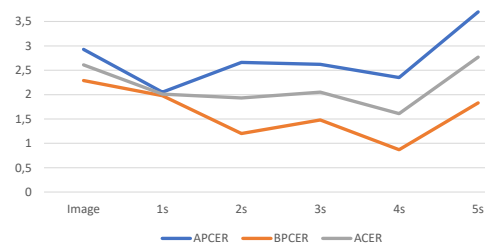


Fig. 3: Study on short/long-range spatio-temporal attention.

Short/long-range spatio-temporal attention. From Figure 3, we can see that the short spatial attention within an image within an image (the start of the grey curve) performs much worse than long spatio-temporal attention over frames spanning a video of 4 seconds in terms of ACER for face PAD. The more frames we use the better performance we gain until the length of video attains 4 seconds. This shows that the model strongly over-fitted the noise when the video is long ($25\text{fps} \times 4\text{s}$).

Table 3: The results of the evaluation on the OULU-NPU dataset. Best results are marked in **bold** and second best in underline.

Prot.	Method	APCER(%)	BPCER(%)	ACER(%) \downarrow
1	Auxiliary [17]	1.6	1.6	1.6
	SpoofTrace [2]	0.8	1.3	1.1
	FAS-SGTD [4]	2.0	0.0	1.0
	CDCN [26]	0.4	1.7	1.0
	DC-CDN [3]	0.5	0.3	<u>0.4</u>
	ViTransPAD (Ours)	0.4	0.2	0.3
2	Auxiliary [17]	2.7	2.7	2.7
	SpoofTrace [2]	2.3	1.6	1.9
	FAS-SGTD [4]	2.5	1.3	1.9
	CDCN [26]	1.5	1.4	1.5
	DC-CDN [3]	0.7	1.9	<u>1.3</u>
	ViTransPAD (Ours)	2.0	0.4	1.2
3	Auxiliary [17]	2.7 \pm 1.3	3.1 \pm 1.7	2.9 \pm 1.5
	SpoofTrace [2]	1.6 \pm 1.6	4.0 \pm 5.4	2.8 \pm 3.3
	FAS-SGTD [4]	3.2 \pm 2.0	2.2 \pm 1.4	2.7 \pm 0.6
	CDCN [26]	2.4 \pm 1.3	2.2 \pm 2.0	2.3 \pm 1.4
	DC-CDN [3]	2.2 \pm 2.8	1.6 \pm 2.1	1.9\pm1.1
	ViTransPAD (Ours)	3.1 \pm 3.0	1.0 \pm 1.3	<u>2.0\pm1.5</u>
4	Auxiliary [17]	9.3 \pm 5.6	10.4 \pm 6.0	9.5 \pm 6.0
	CDCN [26]	4.6 \pm 4.6	9.2 \pm 8.0	6.9 \pm 2.9
	FAS-SGTD [4]	6.7 \pm 7.5	3.3 \pm 4.1	5.0 \pm 2.2
	DC-CDN [3]	5.4 \pm 3.3	2.5 \pm 4.2	4.0 \pm 3.1
	SpoofTrace [2]	2.3 \pm 3.6	5.2 \pm 5.4	<u>3.8\pm4.2</u>
	ViTransPAD (Ours)	4.4 \pm 4.8	0.2 \pm 0.6	2.3\pm2.4

Table 4: The results of cross-dataset testing protocol on OULU-NPU, CASIA-MFSD, Replay-Attack, and MSU-MFSD.

Method	O&C&I to M	O&M&I to C	O&C&M to I	I&C&M to O
	HTER(%)	HTER(%)	HTER(%)	HTER(%)
Color Texture [27]	28.09	30.58	40.40	63.59
LBP-TOP [28]	36.90	42.60	49.45	53.15
Auxiliary(Depth) [17]	22.72	33.52	29.14	30.17
MMD-AAE [29]	27.08	44.59	31.58	40.98
MADDG [24]	17.69	24.5	22.19	27.98
MDRL [30]	17.02	<u>19.68</u>	20.87	25.02
SSDG-M [31]	16.67	23.11	18.21	25.17
ANRL [25]	<u>10.83</u>	17.85	16.03	<u>15.67</u>
ViTransPAD w/o A (Ours)	16.80	21.27	18.50	20.80
ViTransPAD w/A (Ours)	8.39	23.12	<u>16.83</u>	15.63

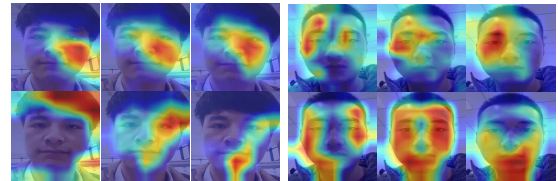
4.4. Intra-/cross-dataset Testing

Table 3 and Table 4 compare the performance of our method with the state-of-the-art methods on OULU-NPU [12] and cross-dataset [24] protocols. We can see that our proposed method ranks first on most protocols of OULU-NPU (i.e., Protocols 1, 2, and 4) and the ‘O&C&I to M’, ‘I&C&M to O’ of cross-dataset testing (‘O&C&M to I’ is the second best closing to the first). Please note that our ViTransPAD can be also integrated in the framework of meta-learning as used in ANRL [25] to further improve the cross-dataset generalization ability. The superior performance shows that our ViTrans can server as an effective new backbone for face PAD.

4.5. Visualization

Due to lack the long-range spatio-temporal dependencies over frames, the short-range attention within a frame is vulnerable to the noise which results its attention maps are less consistent

than the ones of long-range attention either for the liveness or attacks detection as shown in Figure 4. For instance, the upper row of (a) shows that the long-range attention always focus on the left half faces for liveness detection. However, the first attention map of short-range attention (the bottom row of (a)) attends the hairs on the forehead but the succeeding frames switch to focus on the left half faces. The same results can be also observed in the attacks detection as shown in (b).



(a) Liveness

(b) Attack

Fig. 4: Attention maps obtained by GradCAM [32]. Upper row illustrates attention maps of long-range attention over frames and the bottom row shows the ones of short-range attention within a frame.

5. CONCLUSION

We design a Video-based Transformer for face PAD with short/long-range spatio-temporal attention which can not only focus on local details but also the context of a video. The proposed Multi-scale Multi-Head Self-Attention enables the model to learn a fine-grained representation to perform pixel-level discrimination required by face PAD. We also introduce convolutions to our ViTransPAD to integrate desirable proprieties of CNNs which can gain a good computation-accuracy balance. To the best of our knowledge, this is the first approach using video-based transformer for face PAD which can serve as a new backbone for further study.

6. REFERENCES

- [1] Zitong Yu et al., “Deep learning for face anti-spoofing: A survey,” *arXiv preprint arXiv:2106.14948*, 2021.
- [2] Yaojie Liu et al., “On disentangling spoof trace for generic face anti-spoofing,” in *ECCV*, 2020.
- [3] Zitong Yu, Yunxiao Qin, Hengshuang Zhao, Xiaobai Li, and Guoying Zhao, “Dual-cross central difference network for face anti-spoofing,” in *IJCAI*, 2021.
- [4] Zezheng Wang et al., “Deep spatial gradient and temporal depth learning for face anti-spoofing,” in *CVPR*, 2020.

- [5] Junying Gan, Shanlu Li, Yikui Zhai, and Chengyun Liu, “3d convolutional neural network based on face anti-spoofing,” in *ICMIP*, 2017, pp. 1–5.
- [6] Alexey Dosovitskiy et al., “An image is worth 16x16 words: Transformers for image recognition at scale,” *arXiv preprint arXiv:2010.11929*, 2020.
- [7] Anjith George and Sébastien Marcel, “On the effectiveness of vision transformers for zero-shot face anti-spoofing,” in *IJCB*, 2021.
- [8] Zitong Yu et al., “Transrppg: Remote photoplethysmography transformer for 3d mask face presentation attack detection,” *SPL*, 2021.
- [9] Anurag Arnab et al., “Vivit: A video vision transformer,” *arXiv preprint arXiv:2103.15691*, 2021.
- [10] Wenhai Wang, Enze Xie, Xiang Li, Deng-Ping Fan, Kaitao Song, Ding Liang, Tong Lu, Ping Luo, and Ling Shao, “Pyramid vision transformer: A versatile backbone for dense prediction without convolutions,” in *CVPR*, 2021, pp. 568–578.
- [11] Haiping Wu, Bin Xiao, Noel Codella, Mengchen Liu, Xiyang Dai, Lu Yuan, and Lei Zhang, “Cvt: Introducing convolutions to vision transformers,” in *ICCV*, 2021.
- [12] Zinelabinde Boulkenafet, Jukka Komulainen, and et al., “Oulu-npu: A mobile face presentation attack database with real-world variations,” in *FG*, 2017.
- [13] Zhiwei Zhang et al., “A face antispoofing database with diverse attacks,” in *ICB*, 2012, pp. 26–31.
- [14] Ivana Chingovska et al., “On the effectiveness of local binary patterns in face anti-spoofing,” in *Biometrics Special Interest Group*, 2012, pp. 1–7.
- [15] Di Wen, Hu Han, and Anil K Jain, “Face spoof detection with image distortion analysis,” *IEEE TIFS*, 2015.
- [16] Zuheng Ming et al., “A survey on anti-spoofing methods for facial recognition with rgb cameras of generic consumer devices,” *Journal of Imaging*, vol. 6, no. 12, pp. 139, 2020.
- [17] Yaojie Liu et al., “Learning deep models for face anti-spoofing: Binary or auxiliary supervision,” in *CVPR*, 2018.
- [18] Zitong Yu et al., “Face anti-spoofing with human material perception,” in *ECCV*, 2020.
- [19] Zitong Yu, Jun Wan, Yunxiao Qin, Xiaobai Li, Stan Z Li, and Guoying Zhao, “Nas-fas: Static-dynamic central difference network search for face anti-spoofing,” *TPAMI*, 2020.
- [20] Ashish Vaswani et al., “Attention is all you need,” in *NIPS*, 2017.
- [21] Ze Liu et al., “Swin transformer: Hierarchical vision transformer using shifted windows,” in *ICCV*, 2021.
- [22] Hugo Touvron, Matthieu Cord, Matthijs Douze, Francisco Massa, Alexandre Sablayrolles, and Hervé Jégou, “Training data-efficient image transformers & distillation through attention,” in *ICML*, 2021.
- [23] Xizhou Zhu, Weijie Su, Lewei Lu, Bin Li, Xiaogang Wang, and Jifeng Dai, “Deformable detr: Deformable transformers for end-to-end object detection,” *arXiv preprint arXiv:2010.04159*, 2020.
- [24] Rui Shao et al., “Multi-adversarial discriminative deep domain generalization for face presentation attack detection,” in *CVPR*, 2019.
- [25] Shubao Liu, Ke-Yue Zhang, Taiping Yao, Mingwei Bi, Shouhong Ding, Jilin Li, Feiyue Huang, and Lizhuang Ma, “Adaptive normalized representation learning for generalizable face anti-spoofing,” in *ACM MM*, 2021, pp. 1469–1477.
- [26] Zitong Yu et al., “Searching central difference convolutional networks for face anti-spoofing,” in *CVPR*, 2020.
- [27] Zinelabidine Boulkenafet et al., “Face spoofing detection using colour texture analysis,” *IEEE TIFS*, 2016.
- [28] Tiago de Freitas Pereira et al., “Face liveness detection using dynamic texture,” *EURASIP Journal on Image and Video Processing*, 2014.
- [29] Haoliang Li et al., “Domain generalization with adversarial feature learning,” in *CVPR*, 2018.
- [30] Guoqing Wang et al., “Cross-domain face presentation attack detection via multi-domain disentangled representation learning,” in *CVPR*, 2020.
- [31] Yunpei Jia et al., “Single-side domain generalization for face anti-spoofing,” in *CVPR*, 2020.
- [32] Ramprasaath R Selvaraju, Michael Cogswell, Abhishek Das, Ramakrishna Vedantam, Devi Parikh, and Dhruv Batra, “Grad-cam: Visual explanations from deep networks via gradient-based localization,” in *ICCV*, 2017.